Reducing Fluctuations in Slow-Extraction Beam Spill Using Transit-Time-Dependent Tune Modulation

R. Singh,* P. Forck, and S. Sorge
GSI Helmholtz Centre for Heavy Ion Research, Darmstadt, Germany

(Received 29 July 2019; revised manuscript received 19 February 2020; accepted 31 March 2020; published 29 April 2020)

Slow extraction of beams from synchrotrons or storage rings as required by many fixed target experiments is performed by controlled excitation and feeding of a structural lattice resonance. Due to the sensitive nature of this resonant extraction process, the temporal structure of the extracted beam is modulated by the minuscule current fluctuations present on the quadrupole magnet power supplies. Such a modulation leads to pile-up in detectors and significant reduction in accumulated event statistics. This contribution proposes and experimentally demonstrates that by introduction of a further modulation on quadrupole currents with a specific amplitude and frequency, the influence of inherent power supply fluctuations on spill is mitigated. The slow-extraction beam dynamics associated with this method are explained along with the operational results.

DOI: 10.1103/PhysRevApplied.13.044076

I. INTRODUCTION

Controlled slow extraction of beams from synchrotrons and storage rings is required by a host of "fixed target experiments" as well as hadron cancer therapy based on charged particle deposition on tumors [1]. The extracted beam is also referred to as "spill." The extraction procedure is performed in two steps: (a) exciting a lattice resonance and (b) feeding the excited resonance by moving the betatron tunes of individual particles towards it. While most synchrotron facilities drive a horizontal third-order resonance for slow extraction using sextupolar fields [2], there exist a few variants of resonance feeding mechanisms (under operation) such as quadrupole driven [2], betatron-core driven [2], or rf knockout [3,4]. The choice of resonance feeding mechanisms is determined by extraction parameters such as beam energy, instantaneous momentum spread, total spill duration, and macroshape as required by experiments, and, in the case of therapy machines, the ability to swiftly interrupt the extraction process is also vital [2,4]. Accelerator users often assume that the particle count distribution in the spill is solely governed by Poisson statistics. However, with experience, most facilities and users have realized that the minuscule ripples and noise ($< \Delta I/I \approx 10^{-5}$) on currents supplied to focusing quadrupole magnets lead to significant temporal modulation of the extracted spills. These modulated spills are detrimental to the quality of data recorded by experiments, where as much as 2/3 of the delivered beam has been reported to be unusable [5]. Any improvement in the power supply either is deemed to be technologically unfeasible or would lead to long disruption in the operation of a facility. Similarly, the beam delivery systems in hadron cancer therapy synchrotrons are required to provide prescribed irradiation doses with specified beam energy based on the heterogeneity and depth of tumor voxels [6]. Patient safety measures place stringent tolerances on voxel dosages in order to avoid any overdosage, which typically translates into a requirement towards the extracted spill uniformity provided by the synchrotron. Nonuniform spills increase treatment times either due to the treatment by many subsequent low-intensity dose deliveries [7] or due to frequent interlocks produced by safety systems in response to fluctuations in the measured spill before delivery to a patient [8]. Therefore several efforts are being made towards approaches for the reduction of the intensity fluctuations in spills for various medical facilities [7–10].

In order to deal with spill nonuniformities, the primary resonance feeding mechanisms in most facilities (discussed earlier) have been augmented by other techniques. One of the first such techniques found in the literature was proposed at CERN [11], where the resonance feeding mechanism was assisted by a longitudinal stochastic noise, such that the particles were fed at a speed faster than the separatrix modulation induced by power supply noise. This "stochastic extraction" method reduced the effect of power supply ripples and was shown to work well for very long extraction times (several minutes or more) [12,13]. Other ideas also involved some form of longitudinal gymnastics such as "rf phase displacement" [14], "rf channeling" [2], and bunched beam extraction [15], which all reduce the effect of power supply ripples at the cost of rf frequency

*r.singh@gsi.de

modulation of the spill. Although these techniques reduce low-frequency modulations of the spill, they actually hinder experiments that rely on smooth structure at time scales comparable to or smaller than the rf period. Spill smoothing based on feedback systems [16] is nontrivial to operate, given that the slow-extraction transfer function consists of an inherent dynamic delay of the order of milliseconds between particle extraction and measurement. Feedback and servo systems have thus shown improvement only in the low-frequency or macrospill regime (< 50 Hz) [17] and limited success is reported in the literature for the microspill regime (> 50 Hz) [18].

In this paper, we approach the problem of uneven spill structure by primarily influencing the particle transit time, i.e., the time required by a particle to reach the electrostatic septum after it first becomes unstable. The instantaneous variation of transit times for particles due to different initial phase space coordinates and momenta being extracted at the same time instant form a "transit time distribution" of a certain width, which is thus modified. The discussed method is based on controlled tune modulation in correlation with the parameters of transit time distribution.

This method, while smoothing the spill structure against power supply ripples, does not introduce any significant additional longitudinal structure at higher frequencies. The first application of this approach is demonstrated with respect to the quadrupole-driven resonance feeding mechanism, where the effect of power supply fluctuations on spill is expected to be the strongest [2]. The recently concluded High Acceptance Di-Electron Spectrometer (HADES) experiment [19] reported a 50% increase in recorded events compared to previous campaigns [5] as a direct result of the use of this method.

II. THEORETICAL DESCRIPTION

For the theoretical description of the aforementioned technique, we have utilized the Proton Ion Medical Machine Study (PIMMS) [2] notations wherever possible. Figure 1(a) shows the triangular stable phase space area that is characteristic for the application of a one-dimensional third-order resonance as shown in the Kobayashi theory [20].

$\vec{X} \equiv (X, X')$ is a phase space vector with the normalized coordinates

$$X = \frac{x}{\sqrt{\beta_x}} \quad \text{and} \quad X' = \sqrt{\beta_x}x' + \frac{\alpha_x}{\sqrt{\beta_x}}x, \tag{1}$$

where α_x, β_x are the Twiss parameters. The size of the phase space area is defined by unstable fixed points of betatron motion and is given as

$$A_{\text{stable}} = \frac{4\sqrt{3}\pi^2}{3}\left(\frac{\varepsilon_Q}{S_v}\right)^2, \tag{2}$$

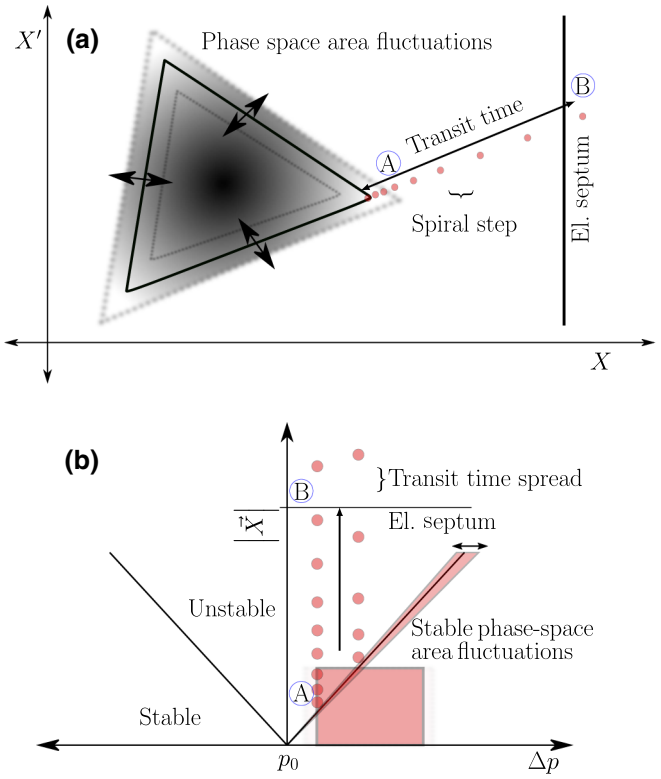

FIG. 1. (a) Schematic showing stable phase space area modulation due to power supply ripples for any specific tune and the transit of particles towards the septum. (b) Steinbach diagram showing the spread in transit times due to amplitude and momentum distribution of fed particles.

where $\varepsilon_Q = 6\pi(Q_m - Q_r)$ is the difference between machine and resonance tunes. S_v is the strength of a virtual sextupole created by an arrangement of N sextupoles governed by the relation

$$S_v e^{3i\psi_v} = \sum_n S_n e^{3i\psi_n} \tag{3}$$

with the normalized sextupole strength of the nth sextupole

$$S_n = \frac{1}{2}\beta_{x,n}^{3/2}(k_2 L)_n \tag{4}$$

and the phase advance ψ_n between the considered location, which is usually that of the electrostatic septum and the location of the nth sextupole. $(k_2 L)_n$ is the integrated focusing strength of the nth sextupole. ψ_v determines the orientation of the stable phase space area. The Steinbach diagram in Fig. 1(b) shows the separation of stable and unstable areas as a function of particle momentum Δp. The slope of the separating line is

$$\left|\vec{X}\right| / \Delta p \propto (Q_r \xi)/(p_0 S_v), \tag{5}$$

where

$$\xi = \left(\frac{\Delta Q}{Q}\right) / \left(\frac{\Delta p}{p}\right) \tag{6}$$

is the chromaticity in the plane of extraction and p_0 is the momentum of a zero-amplitude particle at resonance tune Q_r.

In a typical quadrupole-driven extraction, the stable phase area is slowly shrunk with time by moving the machine tune Q_m towards resonance Q_r such that the particles (starting from larger amplitudes/action) leave the stable area and traverse towards the extraction septum. Upon crossing the electrostatic septum, particles obtain a kick such that the particle trajectory passes through another magnetic kicker, before "spilling" out of the synchrotron. For a particle with a certain amplitude $|\vec{X}|$, the transit time $T_{\rm tr}$ is primarily determined by the distance to resonance ε_Q at which the particle becomes unstable because $T_{\rm tr} \propto 1/\varepsilon_Q$ for $Q_m \to Q_r$ (Eq. 4.17 in Ref. [2]). This relation is a simple manifestation of the following: since the nonlinear sextupolar fields are driving the resonance, the particles starting at lower amplitudes will take longer to transit out of the synchrotron after becoming unstable. From the requirement of a defined size of the stable phase space area, it follows from Eq. (2) that $\varepsilon_Q \propto S_v$. For a particle beam with a given emittance and momentum spread, there is a corresponding distribution in the transit times. The distribution can be characterized by the mean $\overline{T_{\rm tr}}$ and spread $\Delta T_{\rm tr}$. A peculiarity of the transit time distribution is that the transit time spread $\Delta T_{\rm tr}$ is correlated with the mean transit time $\overline{T_{\rm tr}}$ as follows:

$$\overline{T_{\rm tr}} \propto \frac{1}{\overline{\varepsilon_Q}} \quad \text{and} \quad \Delta T_{\rm tr} = \frac{dT_{\rm tr}}{d\varepsilon_Q}\Delta\varepsilon_Q \propto \frac{1}{\overline{\varepsilon_Q}^2}\Delta\varepsilon_Q, \tag{7}$$

as discussed in detail in Ref. [21]. The spiral step at any time step is given as a function of sextupole field strength and coordinates in the previous time step (X_0, X_0') as

$$\Delta X_1 \propto S_v X_0' \left(3^{1/4}\sqrt{A_{\rm stable}}/2 + 1.5X_0\right). \tag{8}$$

The effect of fluctuations on the measured spill structure is illustrated in Fig. 2. The black dashed line in Fig. 2 (bottom) represents the controlled shrinkage of the stable phase space area as it occurs over time, while the solid black line depicts the undesired modulation $\delta A_{\rm stable}$ due to quadrupole field fluctuations for particles with a specific momentum. The nature of fluctuations is similar irrespective of particle momentum, although the absolute stable phase space area is different for different momenta as indicated in Fig. 1(b). As the stable area shrinks, particles leave the stable area in chunks due to $\delta A_{\rm stable}$ fluctuations and their relative counts are depicted in Fig. 2 (middle) shortly after crossing their respective momentum-dependent separatrices denoted by

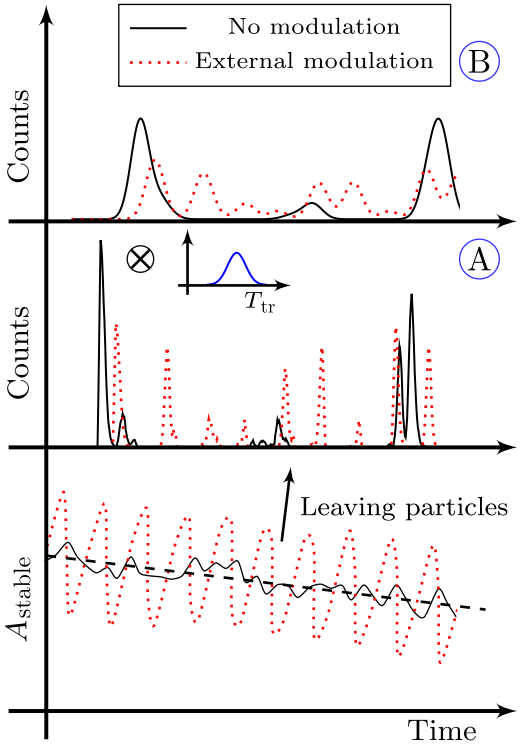

FIG. 2. Bottom: stable phase space area modulation due to inherent power supply ripples (black solid lines) and when external ripples are introduced on quadrupoles (red dotted lines). Middle: spill just after crossing the separatrix, point A in Fig. 1. Top: spill at the measurement location, point B in Fig. 1, after convolution with transit time distribution.

point A (also shown in Fig. 1). Following that, flux of released particles is convolved with the instantaneous transit time distribution $\Delta T_{\rm tr}$ while traversing from point A to point B [Fig. 2 (top)], which can be seen as the point of "spill measurement" or "user experiment." The convolution has the effect of low-pass filtering and frequency components above a certain cutoff frequency $f_{\rm cut} \propto 1/\Delta T_{\rm tr}$ are suppressed.

III. SIMULATION EXAMPLE

The transit time distribution parameters, i.e., $\overline{T_{\rm tr}}$ and $\Delta T_{\rm tr}$, primarily depend on the slow-extraction settings that in turn are determined by the beam parameters, i.e., emittance, energy and its spread, as well as length of spill as elaborated in Refs. [21,22]. An imprint of the transit time spread $\Delta T_{\rm tr}$ can be seen on the spill spectrum by means of the cutoff frequency $f_{\rm cut}$, while $\overline{T_{\rm tr}}$ is expected to scale with $\Delta T_{\rm tr}$ in accordance with Eq. (7). Figure 3 shows the evaluated transit time distributions from particle tracking simulations during a typical spill for the SIS-18 synchrotron at GSI. The energy applied for a C^{6+} beam is 300 MeV/u, where 10^5 test particles are extracted in 0.55 s. The virtual sextupole strength is $S_v = 5.5\ \mathrm{m}^{-1/2}$

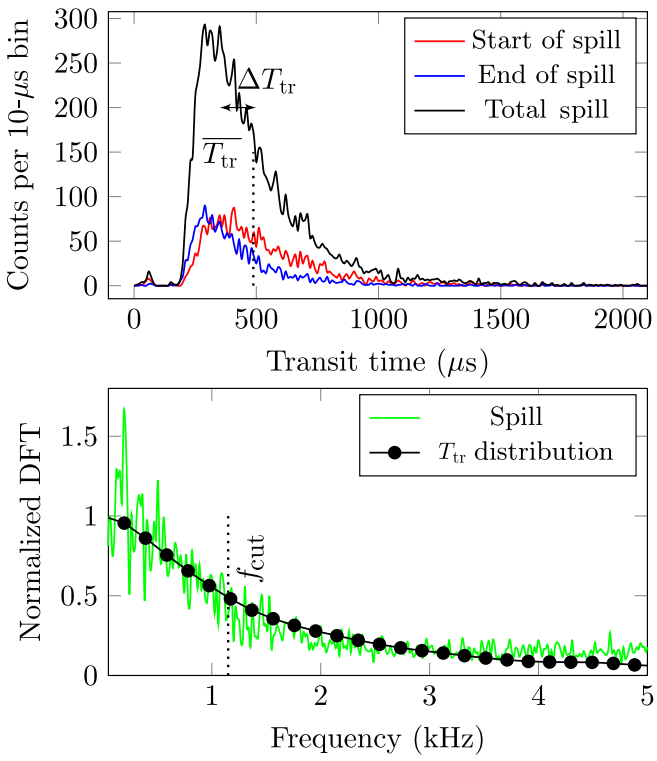

FIG. 3. Simulated transit time distribution (top) and the comparison of its normalized spectrum with the corresponding spill spectrum (bottom).

and the tune Q_x is driven from 4.327 across the third-order resonance 4.33. A revolution time of 1.1 μs, momentum spread $\Delta p/p_0 = 5 \times 10^{-4}$ (2σ), and natural chromaticity $\xi = -0.94$ are applied. In addition, a band limited white noise signal with the relative rms amplitude of 10^{-5} and frequencies in the range (0–9) kHz is introduced into the focusing strengths of the quadrupoles. Mean $\overline{T_{\rm tr}}$ and spread $\Delta T_{\rm tr}$ of the distribution evolve during the spill. Figure 3 (top) shows the transit time distributions at the start and end of the spill, as well as the "total" transit time distribution. The mean and spread are positively correlated $\overline{T_{\rm tr}} \propto \Delta T_{\rm tr}$ in each of those distributions. Unless specified, we discuss the "total" transit time distribution. The mean transit time $\overline{T_{\rm tr}}$ of the "total" transit time distribution is 488 μs. The transit time spread is estimated from its filtering effect in the frequency domain. Figure 3 (bottom) shows the normalized discrete Fourier transform (DFT) of the transit time distribution along with the respective spill spectrum. The spectra are normalized to the value of the second frequency bin of the respective discrete Fourier transforms. Since the transit time distribution resembles an exponential decay as shown in Fig. 3 (top), $\Delta T_{\rm tr}$ can be recovered from the frequency corresponding to half maximum in its Fourier transform [Fig. 3 (bottom)], i.e., $\Delta T_{\rm tr} = 1/(2\pi f_{\rm cut}) = 138$ μs.

IV. COMPARISON WITH MEASUREMENTS

In our method, we apply external modulation frequency $f_{\rm ext}$ with amplitudes larger than the inherent ripples into the quadrupole power supplies with a scheme discussed in Ref. [23]. This leads to a modulation of machine tune Q_m and thus the stable phase space area as marked with a red dotted line in Fig. 2 (bottom).

The spill smoothing works as follows: due to the relatively large externally introduced tune modulation compared to inherent ripples, particles undergo a forced release from the stable phase space area at the applied modulation frequency [Fig. 2 (middle)]. The introduced modulation prevents the lower frequency inherent ripples from "feeding" on the particles, which is in principle similar to a fast separatrix crossing in the rf-based methods [14] and thus inherent lower frequency ripples are strongly suppressed.

In order to ensure that the spill does not form a significant modulation at the introduced frequency, it has to be higher than the cutoff frequency $f_{\rm ext} > f_{\rm cut}$. The upper limit on the introduced frequency is given by the condition that the particles are not recaptured in the other half of the oscillation period. These conditions hint at a certain scaling of the introduced frequency with the mean transit time $f_{\rm ext} \propto 1/\overline{T_{\rm tr}}$ and therefore $f_{\rm cut}$.

Figure 4 shows the simulation and experimental results of the dependence of spill quality on the excitation amplitude and frequency. The weighted duty factor F_W is the weighted sum (with $\langle N_k \rangle$) of duty factors

$$F_k = \langle N_k \rangle^2 / \langle N_k^2 \rangle \tag{9}$$

calculated along the spill for each kth "characterization time interval" $T_c = 10$ ms. N_k is an array of particles counted within each T_c with measurement resolution $T_m = 10$ μs [23]. The extraction parameters are the same as discussed earlier for both simulations and experiments. The main difference between the settings is that the experimental extraction rate is 10^6/s. Another major difference between experiment and simulation is that in the latter, the excitations are of the assumed strength, which is not necessarily true in experiments especially for higher amplitudes and frequencies. Since the present power supplies are not designed to work with these frequencies, there remains an uncertainty in the response of the power supply control system in this regime. The excitation strength that the beam actually receives is expected to be lower than the set excitation. A further unknown quantity is the damping of a high-frequency signal by eddy currents within the beam pipe, which would lower the signal strength at the beam. Therefore the case of the ratio $I_{\rm ex}/I_{600\ \rm Hz} = 15$ for experiments only depicts the set value, and the actual value would be lower. There are two clear trends: the optimal excitation frequency is at approximately 4 times the cutoff frequency (experiments and simulations with other cutoff frequencies show a scaling as discussed in Ref. [22]) and

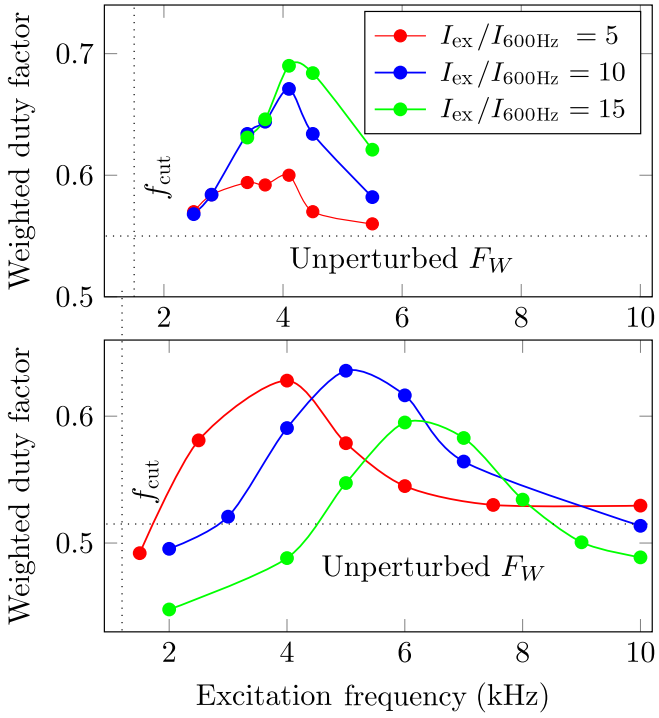

FIG. 4. Weighted duty factor in experiments (top) and simulations (bottom) as a function of excitation frequency and amplitude.

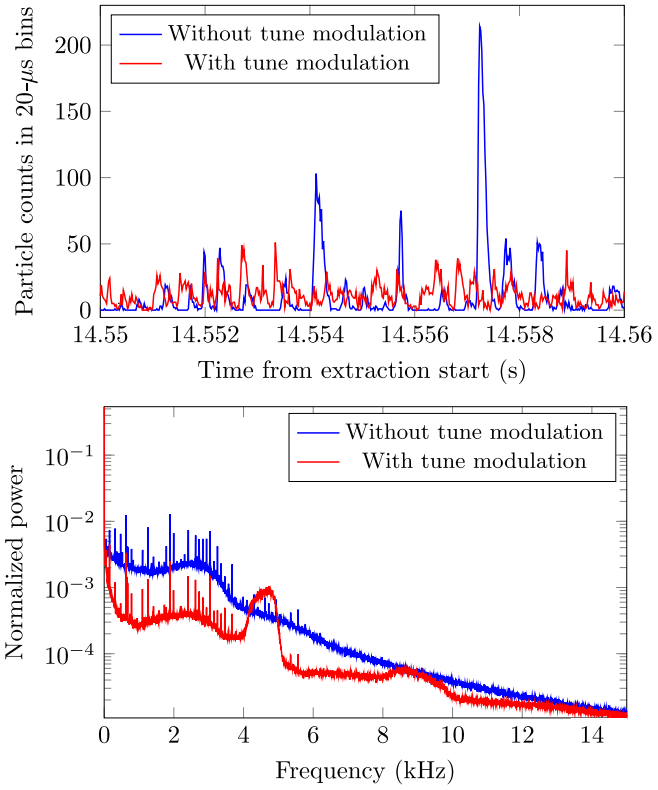

FIG. 5. Comparison of beam spills (top) and their normalized power spectra (bottom) with and without external modulation of tune.

there is a dependence between amplitude and frequency of the introduced modulation.

The first observation establishes the relation between transit time spread and optimal frequency, i.e., $f_{ext} = (3\text{–}5) \times f_{cut}$, and utilizing the example case of the simulation shown earlier, where $\Delta T_{tr}/\overline{T_{tr}} = 138/488 = 0.28$, one arrives at the useful frequency range $f_{cut} < f_{ext} < (12\text{–}20)/\overline{T_{tr}}$. The amplitude of excitation should be significantly higher than the inherent ripple amplitude such that it forces particle release ahead of inherent ripples. On the other hand, it should be low enough such that particles released in the previous cycle are not recaptured (the same argument as for high-frequency modulation) and the total length of spill is not affected due to associated tune modulation. The optimal value found in simulations is a factor of 10 times higher than the inherent ripple amplitude, which corresponds to 2% of total current change during the slow-extraction tune ramp in our experiment. The amplitude and frequency dependence reported in Fig. 4 is related to a dependence between spiral step and transit time, i.e., for smaller transit times, the spiral step is larger and thus a larger amplitude excitation can be employed without recapturing particles. At much higher frequencies $f_{ext} \gg 1/\overline{T_{tr}}$, most particles will not be able to follow the introduced oscillations of the stable area and no periodic release of particles at the introduced frequency will occur and thus spill quality remains unaffected.

Further, since $\overline{T_{tr}}$ and ΔT_{tr} vary during the extraction in a quadrupole-driven extraction process, the optimal exciting frequency evolves with the distribution parameters. Figure 5 shows the spills and their power spectra (normalized to the first frequency bin value) with and without the application of transit-time-dependent tune modulation technique for a high-energy beam of 1.58 GeV/u Ag^{45+} from the SIS-18 for the HADES experiment [19]. A sweep of excitation frequency from 5 to 3.8 kHz is introduced in order to account for the transit time variation during extraction. As a result, all the lower frequency components are suppressed by approximately 10 dB [Fig. 5 (bottom)] along with an improvement by a factor of 2.5 in the weighted duty factor resulting in a much smoother spill. The swept frequencies and their harmonics are also visible in the spill spectrum.

V. SUMMARY

The transit-time-dependent tune modulation introduced in this report utilizes the transit time distribution to suppress the spill temporal fluctuations. It works with unbunched beams and therefore does not interfere with spill quality on rf time scales unlike other contemporary spill-smoothing methods. Uniform unbunched beam extraction is an important requirement put forward by

high-rate coincidence experiments. The method and the resulting technique discussed here are simple and operationally straightforward. The procedure for application is as follows. First an estimate of the cutoff frequencies at the start and end of spill from the spill spectrum is obtained. Then a frequency sweep that satisfies the conditions for an optimal frequency for the whole spill $f_{cut} < f_{ext} < (3–5) \times f_{cut}$ with an amplitude higher by a factor of 10 in comparison to the inherent ripples is applied to the quadrupole power supplies. Since the complete transit time distribution is not directly accessible in the experiments, some empirical tweaking of amplitude and frequency should be performed to obtain the optimal spill smoothing.

This technique has already been commissioned into operation at the GSI SIS-18 facility reducing the beam-time requirements of many experimental campaigns. Due to its simplicity, the method immediately renders itself to other facilities and experiments which face issues with their microspill uniformity. Hence, it could be worth testing it as an alternative or supplementation to servo spill systems as applied in some medical facilities [8,9].

ACKNOWLEDGMENTS

Horst Welker and Andrzej Stafiniak are gratefully acknowledged for their consistent support in introducing the modulation signal in quadrupole power supplies.

[1] U. Amaldi and G. Kraft, Radiotherapy with beams of carbon ions, Rep. Prog. Phys. **68**, 1861 (2005).

[2] L. Badano, M. Benedikt, P. J. Bryant, M. Crescenti, P. Holy, A. Maier, M. Pullia, and S. Rossi, "Proton-ion medical machine study (PIMMS) part I", CERN/PS/ 99-010 (DI), Geneva (1999).

[3] K. Hiramoto and M. Nishi, Resonant beam extraction scheme with constant separatrix, Nucl. Inst. Meth. **A322**, 154 (1992).

[4] K. Noda, M. Kanazawa, A. Itano, E. Takada, M. Torikoshi, N. Araki, J. Yoshizawa, K. Sato, S. Yamada, H. Ogawa, H. Itoh, A. Noda, M. Tomizawa, and M. Yoshizawa, Slow beam extraction by a transverse RF field with AM and FM, NIM A **374**, 269 (1996).

[5] NUSTAR and HADES/CBM physics case and experience, *Proceedings of the First Slow Extraction Workshop*, https://indico.gsi.de/event/4496/page/6, Darmstadt (2016).

[6] Christian P. Karger and Peter Peschke, RBE and related modeling in carbon-ion therapy, Phys. Med. Biol. **63**, 01TR02 (2017).

[7] A. De Franco, L. Adler, F. Farinon, N. Gambino, G. Guidoboni, G. Kowarik, M. Kronberger, C. Kurfrst, S. Myalski, S. Nowak, M. T. F. Pivi, C. S. Schmitzer, I. Strasik, P. Urschtz, and A. Wastl, in *Proc. of IPAC 2018, Vancouver* (JACoW Publishing, Geneva, Switzerland, 2018).

[8] C. Krantz, T. Fischer, B. Kröck, U. Scheeler, A. Weber, M. Witt, and Th. Haberer, in *Proc. of IPAC 2018, Vancouver* (JACoW Publishing, Geneva, Switzerland, 2018).

[9] H. Caracciolo, G. Balbinot, G. Bazzano, J. Bosser, M. Caldara, A. Parravicini, M. Pullia, and C. Viviane, in *Contr. THOAA01 of Proc. of IPAC 2011, San Sebastian, Spain* (JACoW Publishing, San Sebastian, Spain, 2011).

[10] E. Bressi, L. Falbo, C. Priano, and S. Foglio, in *Proc. of IPAC 2018, Vancouver* (JACoW Publishing, Geneva, Switzerland, 2018).

[11] S. van der Meer, "Stochastic extraction, a low-ripple version of resonant extraction", CERN-PS-AA-78-6 (1978).

[12] H. Stockhorst, U. Bechstedt, J. Dietrich, R. Maier, D. Prasuhn, A. Schnase, H. Schneider, and R. Tölle, in *Proc. of EPAC 1996, Barcelona* (Institute of physics publishing, Spain, 1996).

[13] W. Hardt, "Moulding the noise spectrum for much better ultra slow extraction", CERN/PS/DL/LEAR note 84–2.

[14] R. Cappi and Ch. Steinbach, Low frequency duty factor improvement for the CERN PS slow extraction using RF phase displacement techniques, IEEE. Trans. Nucl. Sci. **NS-28** (Vienna, Austria, 1981).

[15] P. Forck, H. Eickhoff, A. Peters, and A. Dolinskii, in *Proc. of EPAC 2000, Vienna* (2000).

[16] H. Sato, T. Toyama, K. Marutsuka, and M. Shirakata, in *Proc. Of the 9th Symp. On Acc. Sci. & Tech, Tsukuba* (KEK, Tsukuba, 1993), Vol. 25.

[17] C. Schoemers, E. Feldmeier, J. Naumann, R. Panse, A. Peters, and T. Haberer, The intensity feedback system at Heidelberg Ion-Beam therapy centre, NIM A **795**, 92 (2015).

[18] J. Shi, J.-C. Yang, J.-W. Xia, Y.-J. Yuan, R.-S. Mao, W.-P. Chai, J. Li, and D. Y. Yin, Feedback of slow extraction in CSRm, NIM-A **714**, 105 (2013).

[19] The HADES colaboration, The high-acceptance dielectron spectrometer HADES, Eur. Phys. J. A **41**, 243 (2009).

[20] Y. Kobayashi and H. Takahashi, Improvement of the emittance in the resonant beam ejection, Proc. Vth Int. Conf. on High Energy Acc. 347 (1967).

[21] S. Sorge, P. Forck, and R. Singh, Measurements and simulations of the spill quality of slowly extracted beams from the SIS-18 synchrotron, J. Phys.: Conf. Ser. **1067**, 052003 (2018).

[22] R. Singh, P. Forck, and S. Sorge, Smoothing of the slowly extracted coasting beam from a synchrotron, arXiv:1904.09195 2019).

[23] R Singh, P. Forck, P. Boutachkov, S. Sorge, and H. Welker, Slow extraction spill characterization from micro to millisecond scale, J. Phys.: Conf. Ser. **1067**, 072002 (2018).